Analytical model of a particular type of positive displacement blower

GIOVANNI MIMMI and PAOLO PENNACCHI
Dipartimento di Meccanica Strutturale, Università degli studi di Pavia,
Via Ferrata 1, I-27100 Pavia, Italy

Abstract
Many papers exist in literature which deal with the twin-screw compressor; this usually has two different rotors, a male and a female, and is commonly used to produce compressed gas for industrial uses.
However, a different type of positive displacement rotary compressor with two screws is sometimes used; one of its typical applications is in car engine supercharging. Present paper deals with the latter type, which is defined as a two-screw blower. This blower has two identical helical rotors, each with three lobes.
The kinematics and the geometry of the rotors are analysed here, and a complete mathematical model for the rotor is defined. Moreover different possible shapes of the rotors, depending on the design parameters, are analysed and the limitations in the choice of the design parameters are presented. Finally an analysis of the theoretical specific slipping of the rotors is presented, showing which zones of the profile are the most stressed.
This model will be useful for further studies on rotor pressure loads and blower dynamics.

Keywords: rotary compressors, superchargers, gears, 3D analytical model, parametric design.

Notation

C - involute cusp point;
h - limit ratio of r_e and r_p;
M - screw motion matrix;
P_0 - pitch point;
p - screw angular pitch;
R - 3D vector representing surface Σ;
r - 2D vector representing curve Γ;
r_b - base radius;
r_e - tip radius;
r_i - inner radius;
r_p - pitch radius;
S - reference system;
w - relative velocity;
u - velocity;
α - upper limit value for parameter ϑ;

Γ - curve;
γ - angle subtending a half of the tip tooth;
δ - angle subtending a complete involute arc;
ε - angle subtending an involute arc from base to pitch circle;
θ - involute pressure angle;
ϑ - parameter;
Σ - surface;
σ - specific slipping;
τ - tangent in the involute cusp;
Ξ - limit equation;
υ - parameter;
ω - angular velocity.

1 INTRODUCTION

For a better understanding, it may be useful to emphasise some considerations, which will explain the origin of this particular type of machine.
The use of positive displacement blowers, driven by the crankshaft, as supercharging devices in internal combustion motors is not recent. These compressors have not had widespread application, apart from the important exception of racing cars, especially if the diffusion of the turbochargers, where the blower is driven by the exhaust gas turbine, is considered, since this type which have had broad application.

The positive displacement blowers used in autos were usually the Roots type. This type was very simple, but its efficiency was very low, as better explained later, therefore its application was not advisable, especially if one considers that the power needed to drive the blower was usually obtained by the motor shaft.

As far as regards to the industrial applications, some positive displacement blowers, which have a high efficiency, are widely used. These machines are the screw compressors, which are characterised by two rotors, a male and a female, whose profile is rather complex and requires a very accurate machining.

Both Roots blowers and twin screw compressors have positive and negative characteristics. The Roots blowers have equal rotor shape, whose geometry is well known and defined by mathematical curves with simple algebraic expression such as cycloids (**1, 2**) or involutes (**3**). However their efficiency is quite low, as reported by many authors (**4-7**) on the basis of experimental and theoretical studies. Some authors (**7**) have proposed different shapes for the rotors too in order to improve the efficiency.

The twin screw compressors have the rotors characterised by a geometry rather complex that led to several studies about the profile shape optimisation and the development of special design software (**8-14**) in recent years. The complexity of the profile is well expressed in (**10**) where they are defined as "… some kind of recipe, where the ingredients have been points, straight lines and parts of mathematical curves that are mixed in suitable proportions". Moreover there was a certain interest in designing the cutter shape for the machining of the male and female rotors (**15**) with a particular interest in the performances obtained on the basis of a particular cutter shape and of the manufacturing cost. A great advantage of twin screw compressors is their efficiency that is rather high as reported in many studies both theoretical and experimental (**8**, **14-21**). Due to the diffusion of these compressors, some authors have also presented studies about the dynamic effects on the rotors (**22-24**) starting from an analytical model of the rotors.

The blower analysed here merges different characteristics of the two types previously described. The target in this case consists of the combination of the Roots rotor simple geometry on the axial section with the high efficiency of the screw blowers. In fact, this compressor has two identical rotors, such as the Roots type, but with a helical shape, which comes from screw compressors. Since this blower is employed for supercharging internal combustion motors, the performance improvements are usually evaluated in terms of torque or power increasing or emissions reduction rather than efficiency. Several papers stress the performance improvement achieved by this type of blower (**25-27**).

The aim of this paper is to give a 3D analytical model for the rotor shape. The knowledge of this analytical model gives the basis for the study of the dynamic effects of the pressure loads on the rotors. This may be carried out with a method similar to that presented in (**22**, **24**, **28**), which needs the analytical model of the rotors in order to define the contact lines, the sector of surfaces where the pressure acts, etc.

Therefore the main part of present paper will deal with the definition of the analytical model of the rotors by considering the analytical expression of all the surfaces that compose the rotor and discussing the effect of the design parameter changes. Only few considerations will be presented about the generation of the profiles by means a simple rack, since this procedure on one hand can easily explain the generation of the profiles but on the other hand it is not so useful to determine the 3D analytical model of the rotor.

2 ROTOR DESIGN

It is not extremely difficult to define the rotor shape if it is considered that the rotor profiles have to be conjugated and consequently the arcs of curves, which compose the profile, are

likely to belong to a finite set of functions only. Therefore the analysis begins by considering an axial section of the rotors which is shown in Figure 1.

Three reference systems are used: the fixed system S_f and the mobile systems S_1 and S_2, rigidly connected with each rotor and rotating with it. The origins of systems S_1 and S_2 are in the geometric centres of the rotors, while that of S_f is at the midpoint of segment O_1O_2. The absolute rotations of the two mobile reference systems are equal in modulus, but in opposite directions. In Figure 1 a certain likeness between these teeth and the involute gears is evident.

The pitch curves of the kinematic pair are the circumferences $\Gamma_{p1,2}$ with radius r_p (see Figure 1). The pitch point P_0 coincides with the origin of reference system S_f.

Moreover it can be considered that a suitable alternative to the cycloidal form for the blower rotors is the involute form as reported in (**3**). However, in this case the space (❶ in Figure 1) is extremely reduced between the tip of a tooth and the inner part of the vane of the other rotor as compared to standard modular design.
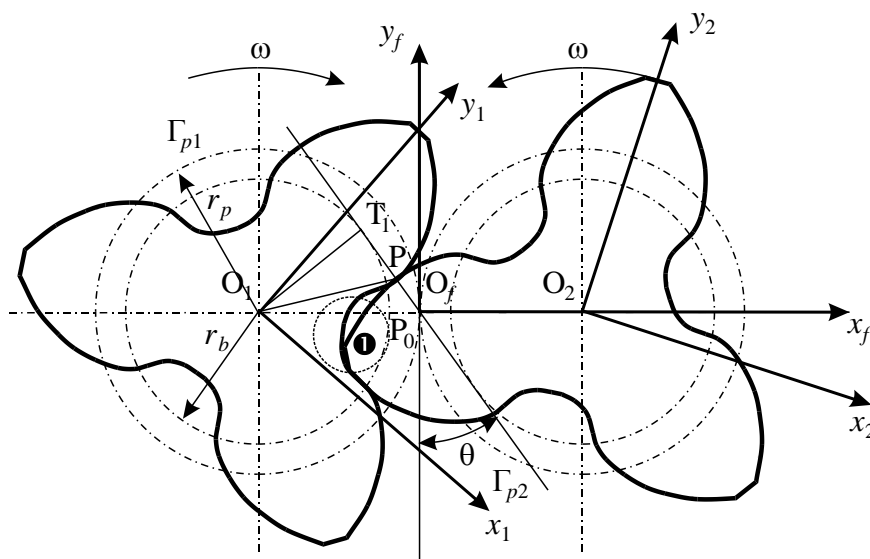

Figure 1. Axial section of two-screw blower rotors.

2.1 Profile generation by rack

As noticed the rotor profile on the axial section presents involute arcs that can be easily obtained by a simple rack (**1**), which is symmetric with respect to x_f and antisymmetric with respect to y_f (Figure 2). This ensures identical profiles on both rotors. If the rack consists of two lines, A-B and B-C, the rack to rotor generation will result in exactly the same profile, but the problem of undercut may arise. In fact, by using a rack only a fixed minimum number of teeth can be obtained avoiding undercut, see f.i. (**29**). In the case reported in Figure 2, n_{min} will be approximately equal to 6. A possible procedure to avoid undercut consists in modifying the rack by means of a convex curve, say a circle, which is put smoothly on the rack between points D and E. So not only will the undercut be conveniently abolished, but also the radius of the curvature can be used as another profile parameter to get a family of rotors in which the optimal profile with respect to displacement and manufacturing may be found.

The consideration of the rack explains the profile generation, but it is also useful to determine the analytic expressions in a parametric form of the curves which compose the profile, therefore a different procedure will be adopted by considering each arc that compose the profile. As a consequence of the symmetry, the analysis is restricted to a half of a tooth.
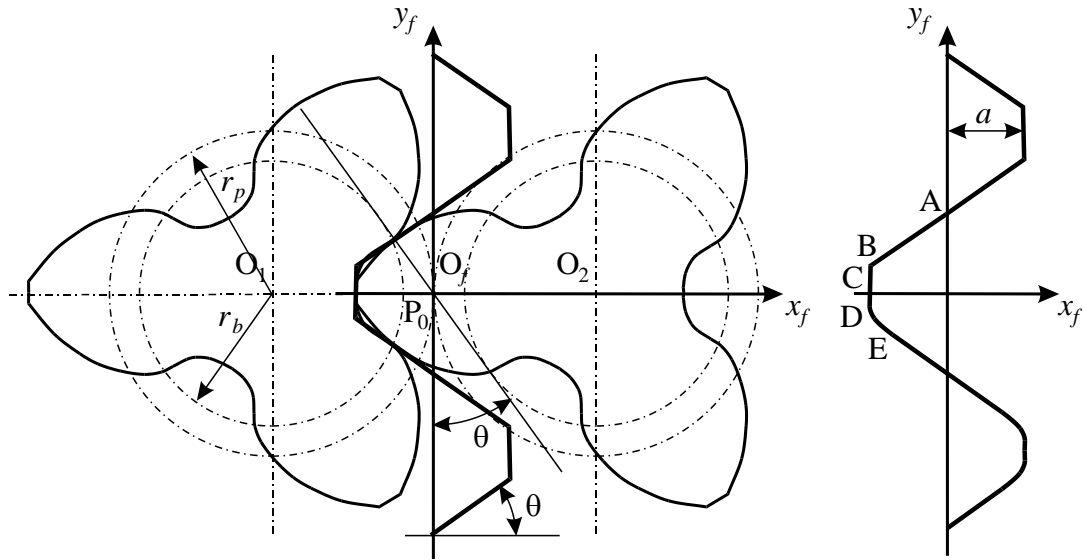
Figure 2. Axial section of two-screw blower rotors.

2.2 Inner and tip circles

Figure 3, which represents a magnification of a rotor half tooth, shows that two arcs of circumference, ① and ②, delimit the tooth. Practically speaking, they correspond to the inner and tip circle of involute gears. So, if the tip radius r_e and the inner radius r_i are defined, the parametric equation of the arcs $\Gamma_{e1,2}$ and $\Gamma_{i1,2}$ in the reference systems S_1 and S_2 is very simple, except for the rotation in the corresponding reference system for the correct angular positioning. The limitation of the parameters ϑ_i and ϑ_e is considered later.
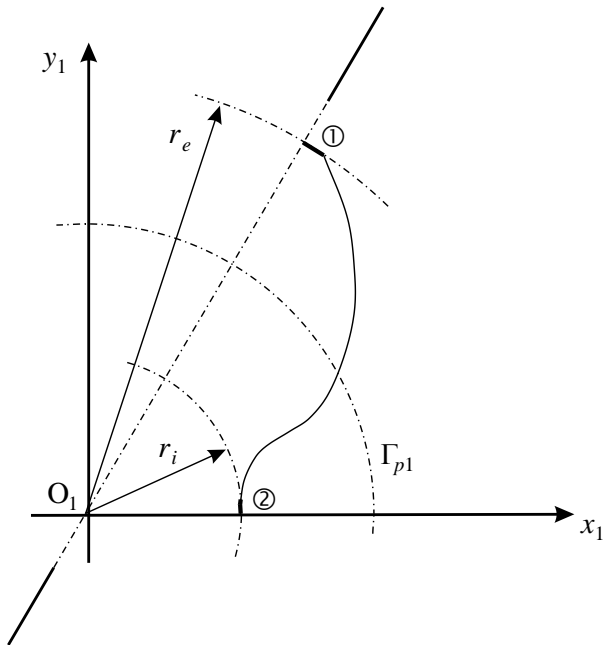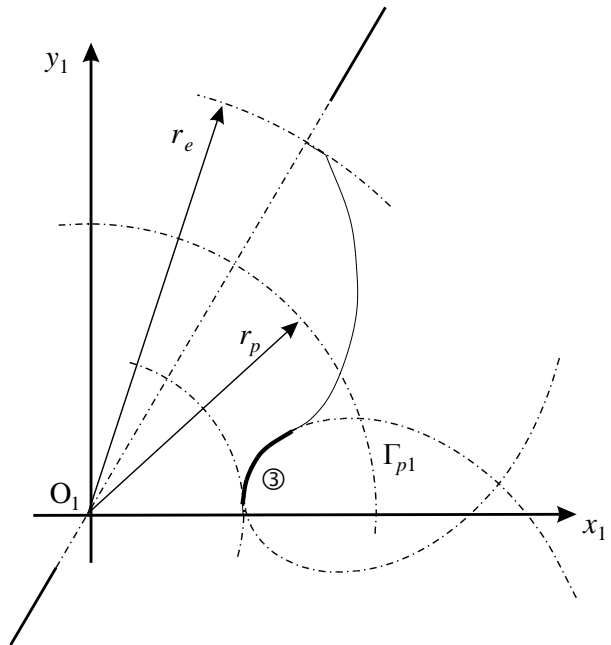

Figure 3. Tip ① and inner ② arcs.

Figure 4. Epitrochoid arc.

$$\Gamma_{e1,2}: \begin{cases} x_{e1,2}\left(\vartheta_{e1,2}\right) = r_e \cos\vartheta_{e1,2} \\ y_{e1,2}\left(\vartheta_{e1,2}\right) = r_e \sin\vartheta_{e1,2} \end{cases} \quad 0 \le \vartheta_{e1,2} \le \alpha_{e1,2} \tag{1}$$

$$\Gamma_{i1,2} : \begin{cases} x_{i1,2}\left(\vartheta_{i1,2}\right) = r_i \cos \vartheta_{i1,2} \\ y_{i1,2}\left(\vartheta_{i1,2}\right) = r_i \sin \vartheta_{i1,2} \end{cases} \quad 0 \leq \vartheta_{i1,2} \leq \alpha_{i1,2} \tag{2}$$

2.3 Epitrochoid arc

During the rotation, the inner and tip arcs are not always in mesh, therefore it is necessary to determine what kind of curve is enveloped by the extreme points of the tip arc of one rotor on the other. The determination of an arc of such a type of curve, labelled by ③ in Figure 4, is a common problem in the study of positive displacement machines and it has been deeply analysed by the authors in (**30-32**) where the analytical expressions are developed. The solution is given by an epitrochoid arc $\Gamma_{epi1,2}$, whose parametric equation in reference systems S_1 and S_2 is:

$$\Gamma_{epi1,2} : \begin{cases} x_{epi1,2}\left(\vartheta_{epi1,2}\right) = 2\,r_p \cos \vartheta_{epi1,2} - r_e \cos 2\vartheta_{epi1,2} \\ y_{epi1,2}\left(\vartheta_{epi1,2}\right) = -2\,r_p \sin \vartheta_{epi1,2} + r_e \sin 2\vartheta_{epi1,2} \end{cases} \quad 0 \leq \vartheta_{epi1,2} \leq \alpha_{epi1,2} \tag{3}$$

Also in this case, the curve is defined except for a rotation around the origin of the relative reference system. The lower limit for the parameter ϑ_{epi} is 0, which corresponds to the extreme of the loop opposite the double point of the curve, while the upper limit α_{epi} will be discussed in the next paragraph.
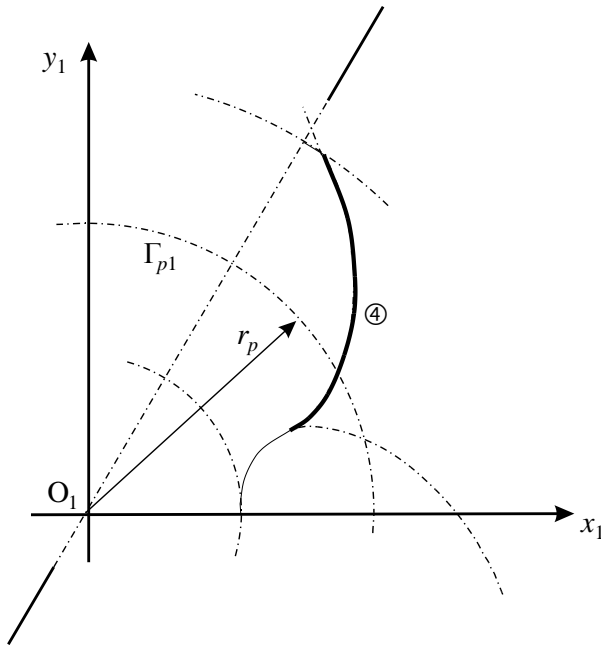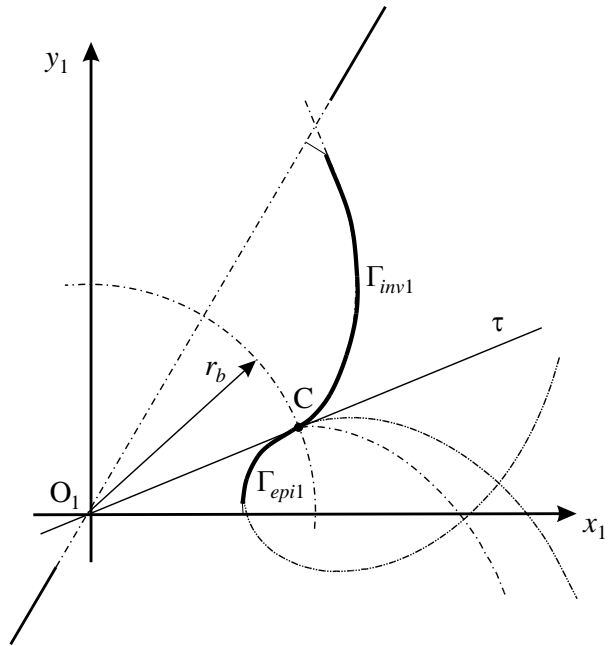

Figure 5. Involute arc.

Figure 6. Involute cusp and tangent in the cusp τ.

2.4 Limits of epitrochoid arc and involute base circle determination

For the complete determination of the rotor profile, only the fourth arc, labelled by ④ in Figure 5, has to be defined. If it is considered that the arc here examined is always and only in mesh with the corresponding arc of the other rotor and that the arcs are equal to each other, it can be inferred that those arcs should be involute arcs (see e.g. **1**, **2**, **33**).

Moreover, the involute has a cusp on its base circle, so the tangent τ in the curve cusp C is radial (see Figure 6).

The latter consideration suggests the criterion for the continuity condition between the involute $\Gamma_{inv1,2}$ and epitrochoid $\Gamma_{epi1,2}$ arcs. The two curves must have the same tangent at the junction point, therefore the tangent to the epitrochoid has to coincide with τ in the fillet between the two arcs; besides it has to pass through the origin $O_{1,2}$ of the related reference system (see Figure 6). This allows us to determine the value of the parameter α_{epi} and the coordinates of the extreme point C of arc $\Gamma_{epi1,2}$. The tangent to curve $\Gamma_{epi1,2}$ in a general point (x_0, y_0) has the following analytic expression:

$$\frac{x_{epi}(\vartheta_{epi}) - x_0}{\dfrac{\partial x_{epi}}{\partial \vartheta_{epi}}} = \frac{y_{epi}(\vartheta_{epi}) - y_0}{\dfrac{\partial y_{epi}}{\partial \vartheta_{epi}}} \tag{4}$$

Considering now that the tangent has to pass through the origin of the reference system, equation (4) becomes:

$$\frac{\left. \dfrac{\partial y_{epi}}{\partial \vartheta_{epi}} \right|_{\vartheta_{epi}=\alpha_{epi}}}{\left. \dfrac{\partial x_{epi}}{\partial \vartheta_{epi}} \right|_{\vartheta_{epi}=\alpha_{epi}}} = \frac{y_{epi}(\alpha_{epi})}{x_{epi}(\alpha_{epi})} \tag{5}$$

By replacing equation (3) and its derivatives in equation (5), the value α_{epi} in closed form as function of r_p and r_e is obtained:

$$\alpha_{epi} = \arccos \frac{r_e^2 + 2 r_p^2}{3 r_e r_p} \tag{6}$$

It is worthwhile noticing that the extreme point C of the arc Γ_{epi}, which has coordinates $(x_{epi}(\alpha_{epi}), y_{epi}(\alpha_{epi}))$, belongs also to the involute base circle Γ_b (see Figure 6). For the previous considerations, the base radius r_b can then be determined as:

$$r_b = \sqrt{x_{epi}^2(\alpha_{epi}) + y_{epi}^2(\alpha_{epi})} = \sqrt{4 r_p^2 + r_e^2 - 4 r_e r_p \cos\alpha_{epi}} = \sqrt{\frac{4 r_p^2 - r_e^2}{3}} \tag{7}$$

A well known relationship between the base radius r_b and the pitch radius r_p for the involute profiles exists, so it is possible to determine the pressure angle θ of the involute and to note that it is not an independent parameter in this case, since it is a function of the radii as shown in equation (7):

$$\theta = \arccos \frac{r_b}{r_p} \tag{8}$$

2.5 Involute arc

Now the equation of the arc $\Gamma_{inv1,2}$, labelled by ④ in Figure 5 can be found out. The parametric expression of the involute is reported for instance in (**2**) and, except for a rotation in the relative reference system S_1 and S_2 for the correct angular positioning, is given by:

$$\Gamma_{inv1,2} : \begin{cases} x_{inv1,2}(\vartheta_{inv1,2}) = r_b \cos\vartheta_{inv1,2} + r_b \vartheta_{inv1,2} \sin\vartheta_{inv1,2} \\ y_{inv1,2}(\vartheta_{inv1,2}) = r_b \sin\vartheta_{inv1,2} - r_b \vartheta_{inv1,2} \cos\vartheta_{inv1,2} \end{cases} \quad 0 \le \vartheta_{inv1,2} \le \alpha_{inv1,2} \tag{9}$$

Evidently the arc $\Gamma_{inv1,2}$ begins on the base circle and ends at the intersection with the tip circle, so the value of the parameter $\alpha_{inv1,2}$ can be obtained by the following equation, and also by considering equation (9):

$$x_{inv}^2(\alpha_{inv}) + y_{inv}^2(\alpha_{inv}) = r_e^2 \quad \rightarrow \quad \alpha_{inv}^2 = \frac{r_e^2 - r_b^2}{r_b^2} \tag{10}$$

Now it is important to evaluate the angle γ which subtends the tip arc $\Gamma_{e1,2}$ and which evidently coincides with the angle subtending the inner arc $\Gamma_{i1,2}$. Note that this value also coincides with the limit values of parameters α_i and α_e. Due to the symmetry, the arc subtended by a half of a tooth on the Γ_p is equal to $\pi/6$ (see Figure 7), while the angle δ subtended by the complete arc Γ_{inv} is equal to:

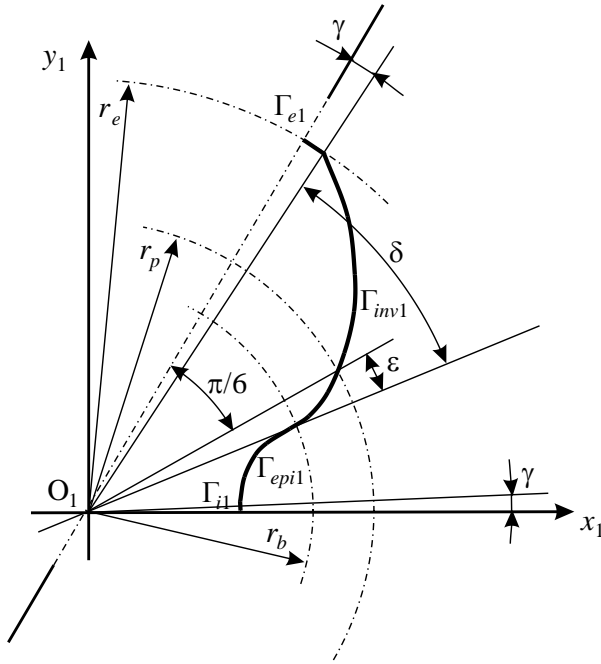$$\delta = \arctan\frac{y_{inv}(\alpha_{inv})}{x_{inv}(\alpha_{inv})} \tag{11}$$
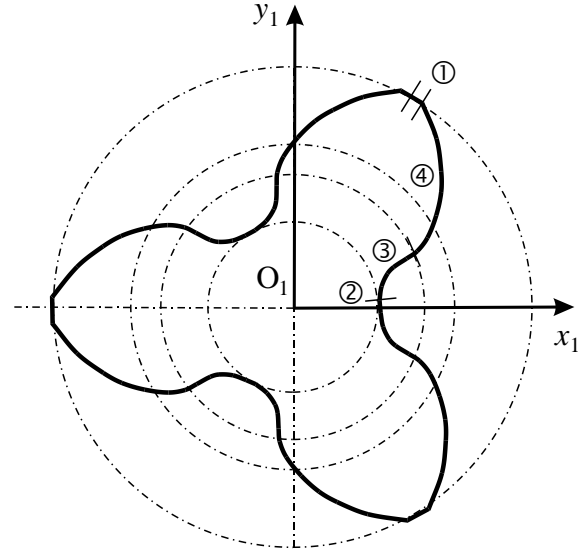

Figure 7. Determination of angle γ.

Figure 8. Complete rotor: ① and ② circumference arcs, ③ epitrochoid arc, ④ involute arc.

We can now determine the value of the parameter ϑ_{inv} which corresponds to the intersection between Γ_{inv} and the pitch circle Γ_p, by using the following:

$$x_{inv}^2(\hat{\vartheta}_{inv}) + y_{inv}^2(\hat{\vartheta}_{inv}) = r_p^2 \quad \rightarrow \quad \hat{\vartheta}_{inv}^2 = \frac{r_p^2 - r_b^2}{r_b^2} \tag{12}$$

and obtain the value of the angle ε, which subtends the involute arc from the base circle Γ_b to Γ_p, as follows:

$$\varepsilon = \arctan \frac{y_{inv}(\hat{\vartheta}_{inv})}{x_{inv}(\hat{\vartheta}_{inv})} \tag{13}$$

Finally angle γ is equal to:

$$\gamma = \frac{\pi}{6} - \delta + \varepsilon \tag{14}$$

The assembly of arcs determined by (1), (2), (3) and (9), with suitable rotations in systems S_1 and S_2, allows us to define the profile of a half tooth and finally, by using symmetry, that of the rotor (see Figure 8).

2.6 Profile determination in 3D space

Once the functions which represent the arcs Γ_i, Γ_e, Γ_{epi} and Γ_{inv} are determined, they can be suitably rotated and the 2D analytical model of the rotor defined as already shown in Figure 8. By starting from the 2D model, it is rather simple to define the 3D model of the rotor too, which is made by the surfaces Σ_i, Σ_e, Σ_{epi} and Σ_{inv}. These are developed from the corresponding arc by a screw motion. For the analytical expression it is first necessary to define the vector $\boldsymbol{r}$, which represents the arc in 2D. By considering for example the epitrochoid, it is:

$$\boldsymbol{r}_{epi}(\vartheta_{epi}) = \begin{bmatrix} x_{epi}(\vartheta_{epi}) & y_{epi}(\vartheta_{epi}) & 0 & 1 \end{bmatrix}^{\mathrm{T}} \tag{15}$$

If p is the angular pitch of the screw rotors, the screw motion matrix $\mathbf{M}(\upsilon)$ is equal to:

$$\mathbf{M}(\upsilon) = \begin{bmatrix} \cos\upsilon & -\sin\upsilon & 0 & 0 \\ \sin\upsilon & \cos\upsilon & 0 & 0 \\ 0 & 0 & 1 & p\upsilon \\ 0 & 0 & 0 & 1 \end{bmatrix} \quad 0 \leq \upsilon \leq \frac{2}{3}\pi \tag{16}$$

In equation (16) it is stressed that the rotors of the compressor under consideration perform only a 120° screw rotation. Therefore surface Σ_{epi} is represented in 3D by $\boldsymbol{R}_{epi}$

$$\Sigma_{epi} : \boldsymbol{R}_{epi}(\vartheta_{epi}, \upsilon) = \mathbf{M}(\upsilon)\boldsymbol{r}_{epi}(\vartheta_{epi}) \tag{17}$$

By reiterating the procedure illustrated previously for all the arcs which compose the rotor section, an analytical model of the rotor is finally obtained as reported in Figure 9.
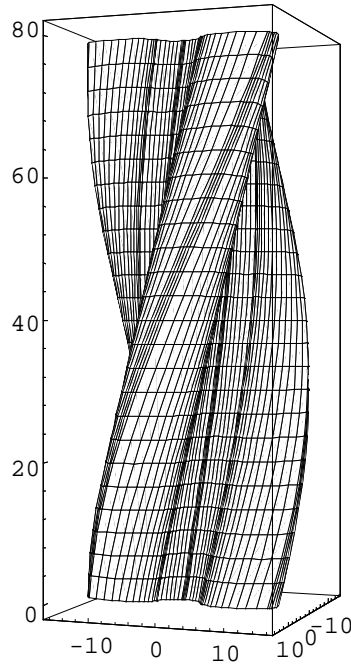
Figure 9. Rotor analytical model.

3 DESIGN PARAMETERS AND LIMITS

A certain likeness between the analysed rotor and the involute gears, as shown in Figure 1 and Figure 8, has already been stressed. However, the low number of teeth of these rotors requires an external synchroniser. Moreover, in this case the concept of modular design cannot be used, because neither an actual addendum nor a dedendum exists. Only two design parameters are independent, among all those which appear in the previous equations: the number of teeth which is usually equal to three and also the inner radius which can be expressed as function of the pitch and tip radius as follows:

$$r_i = 2r_p - r_e \tag{18}$$

The pressure angle θ depends on radii r_p and r_e too, as shown by equation (8). In particular, by rearranging equation (8) it is obtained:

$$r_e = r_p \sqrt{\left(4 - 3\cos^2\theta\right)} \tag{19}$$

The previous expression shows that teeth characterised by the same pressure angle θ are represented in the plane $r_p r_e$ by lines through the origin of equation $r_e = h\, r_p$. These lines characterise similar rotors. Therefore it is suitable to select those two radii as independent design parameters.

Now the limits of the design parameters are discussed. Two boundary values are quite easy to obtain by evaluating the limit shapes of the rotors which correspond to $r_e = r_p$, when the rotor profile turns into a circumference, and to $r_e = 2\, r_p$ when inner radius has a null value. Actually the condition:

$$r_p < r_e < 2\, r_p \tag{20}$$

is too wide, since it does not take the fact that the tooth is sharpened into account, i.e. the angle γ of equation (14) is zero. By again considering equations (10) and (12), and by substituting the value of r_b given by equation (7), it is obtained:

$$\hat{\vartheta}_{inv}^2 = \frac{r_e^2 - r_p^2}{4r_p^2 - r_e^2} \tag{21}$$

$$\alpha_{inv}^2 = \frac{4\left(r_e^2 - r_p^2\right)}{4r_p^2 - r_e^2} = \left(2\hat{\vartheta}_{inv}\right)^2 \tag{22}$$

The angles δ and ε can also have a different expression if the geometric meaning of the involute is considered. As far as regards to Figure 10, the following equations are valid:

$$\overline{OA} = r_b, \quad \overline{AB} = r_b \hat{\vartheta}_{inv}, \quad A\hat{O}B = \arctan \frac{\overline{AB}}{\overline{OA}} = \arctan \hat{\vartheta}_{inv}$$

$$\overline{OC} = r_b, \quad \overline{CD} = r_b \alpha_{inv}, \quad C\hat{O}D = \arctan \frac{\overline{CD}}{\overline{OC}} = \arctan \alpha_{inv} \tag{23}$$

Equations (21), (22) and (23) allow us to determine:

$$\delta = \alpha_{inv} - \arctan \alpha_{inv} = 2\,\hat{\vartheta}_{inv} - \arctan 2\,\hat{\vartheta}_{inv} \tag{24}$$

$$\varepsilon = \hat{\vartheta}_{inv} - \arctan \hat{\vartheta}_{inv} \tag{25}$$
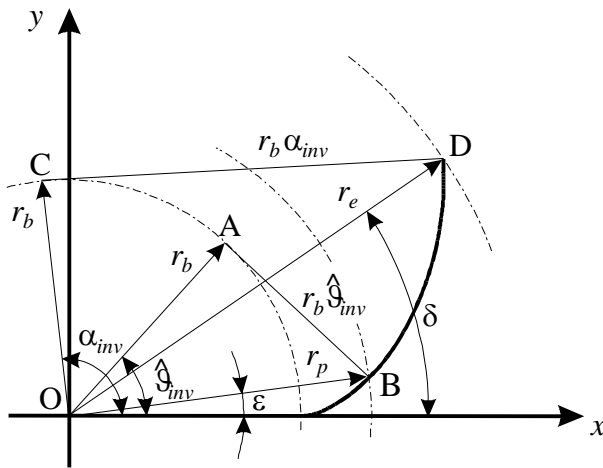

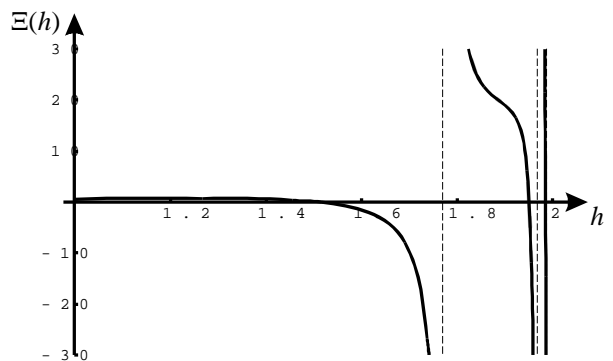Figure 10. Determination of δ and ε.

Figure 11. Representation of limit function $\Xi(h)$.

If the limit condition corresponding to $\gamma = 0$ is evaluated by using equation (14) and replacing equations (24) and (25), one obtains:

$$\frac{\pi}{6} - \hat{\vartheta}_{inv} = \arctan \hat{\vartheta}_{inv} - \arctan 2\hat{\vartheta}_{inv} \tag{26}$$

and by applying the tangent function to both parts of equation (26):

$$\frac{\tan\dfrac{\pi}{6}-\tan\hat{\vartheta}_{inv}}{1+\tan\dfrac{\pi}{6}\tan\hat{\vartheta}_{inv}}=\frac{\hat{\vartheta}_{inv}-2\hat{\vartheta}_{inv}}{1+2\vartheta_{inv}^2}\rightarrow\hat{\vartheta}_{inv}\left(1+\frac{\sqrt{3}}{3}\tan\hat{\vartheta}_{inv}\right)-\left(1+2\vartheta_{inv}^2\right)\left(\frac{\sqrt{3}}{3}-\tan\hat{\vartheta}_{inv}\right)=0 \tag{27}$$

Taking into account that a limit relation such as $r_e = h\,r_p$ is looked for, equation (21) and (27) consequently become:

$$\vartheta_{inv}^2=\frac{h^2-1}{4-h^2} \tag{28}$$

$$\Xi(h)=\sqrt{\frac{h^2-1}{4-h^2}}\left(1+\frac{\sqrt{3}}{3}\tan\sqrt{\frac{h^2-1}{4-h^2}}\right)-\frac{2+h^2}{4-h^2}\left(\frac{\sqrt{3}}{3}-\tan\sqrt{\frac{h^2-1}{4-h^2}}\right)=0 \tag{29}$$

Limit equation $\Xi(h)=0$ is shown in Figure 11. Among the infinite solutions[1] that equation (29) has in the h open interval (1;2), which represents inequality (20), the lower one has to be chosen that is equal to $h = 1.50714$. Therefore the space of the admissible design parameter values becomes (see Figure 12):
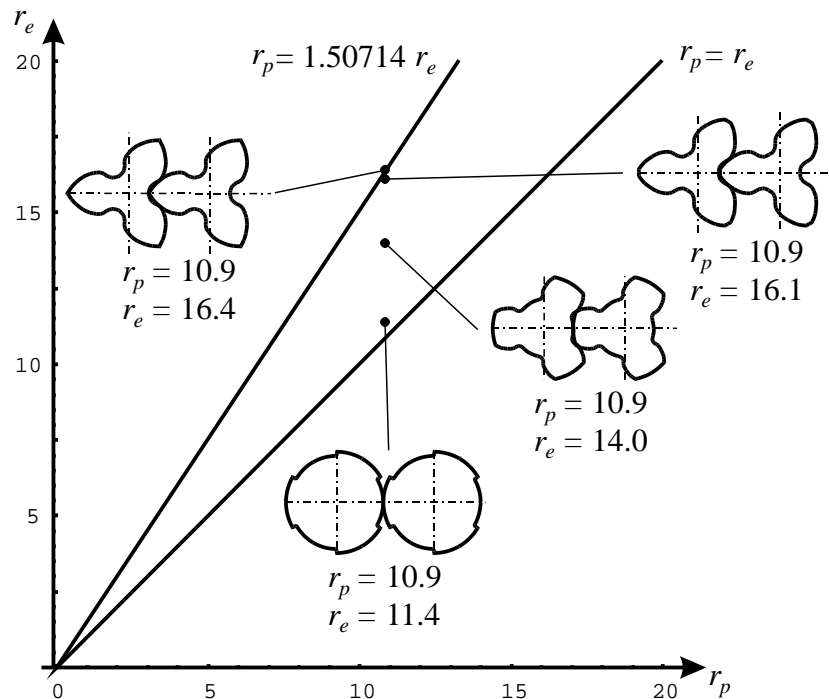
$$r_p < r_e < 1.50714\,r_p \tag{30}$$

Figure 12. Space of design parameter r_p and r_e.

CONCLUSIONS

The present paper deals with the design of a particular type of screw blower rotors. The traditional method for generating the rotor profiles by rack is initially taken into account; it is useful to generate the profiles but it does not give an explicit 3D analytical model of the rotor

---

[1] Point $h = 2$ is a second type discontinuity (**34**) for function $\Xi(h)$, since $\nexists \lim\limits_{h\to 2}\Xi(h)$.

as given by the method presented here. This analytical model is the basis for further studies on the dynamic of the blower rotors.

The analytical model is obtained by considering all the surfaces, which compose the rotor, and giving their parametric expressions. On the basis of the proposed model of the rotors, a study about the design parameters and limits is proposed and parameter space defined.

ACKNOWLEDGEMENTS

REFERENCES

1 **Buckingham, E.** *Analitical Mechanics of Gears*. Dover, New York, 1963.

2 **Litvin, F.L.** *Gear Geometry and Applied Theory*. Prentice-Hall, Englewood Cliffs, NJ, 1994.

3 **Merritt, H.E.** *Gears*. Pitman, London, 1954.

4 **Stone, R.C.** The Efficiency of Roots Compressors and Compressors with Fixed Internal Compression. *Proc Instn Mech Engrs* vol **202** no A3, 1988, 199-205.

5 **Kestin, J.** and **Owczarek, J.A.** The expression of Work in a Roots Blower. *Proc Instn Mech Engrs*, **152-3**, 1B, 1952, 91-94.

6 **Glaister, E.** Communication. *Proc Instn Mech Engrs*, **152-3**, 1B, 1952, 95.

7 **Shu, P.C., Tang, Y.** and **Peng, X.Y.** A substitute of Roots Blower – monotooth rotary compressor. In Proceedings of *1994 International Compressor Engineering Conference at Purdue* (Ed W. Soedel), Purdue University, West Lafayette, Indiana, Vol. 1, 1994, 317-322.

8 **Singh, P.J.** and **Bowman, J.L.** Effect of design parameters on oil-flooded screw compressor performance. In Proceedings of *1986 International Compressor Engineering Conference at Purdue* (Eds J.F. Hamilton and R. Cohen), Purdue University, West Lafayette, Indiana, Vol. 1, 1986, 71-88.

9 **Zenan, X.** and **Dagang, X.** Study on actual profile surface and engaging clearance of screw compressor rotors. In Proceedings of *1986 International Compressor Engineering Conference at Purdue* (Eds J.F. Hamilton and R. Cohen), Purdue University, West Lafayette, Indiana, Vol. 1, 1986, 305-311.

10 **Edström, S.E.** A modern way to good screw rotors. In Proceedings of *1992 International Compressor Engineering Conference at Purdue* (Ed J.F. Hamilton), Purdue University, West Lafayette, Indiana, Vol. 2, 1992, 412-430.

11 **Bennewitz, C.** Software support for screw rotor design, manufacture and quality control. In Proceedings of *1992 International Compressor Engineering Conference at Purdue* (Ed J.F. Hamilton), Purdue University, West Lafayette, Indiana, Vol. 2, 1992, 431-437.

12 **Zhang, L.** and **Hamilton, J.F.** Main geometric characteristics of the twin screw compressor. In Proceedings of *1992 International Compressor Engineering Conference at Purdue* (Ed J.F. Hamilton), Purdue University, West Lafayette, Indiana, Vol. 2, 1992, 449-456.

13 **Zicheng, Z.** Computer aided design of a twin-screw refrigerant compressor. In Proceedings of *1992 International Compressor Engineering Conference at Purdue* (Ed J.F. Hamilton), Purdue University, West Lafayette, Indiana, Vol. 2, 1992, 457-466.

14 **Stosic, N.** and **Hanjalic, K.** Development and optimization of screw engine rotor pairs on the basis of computer modelling. In Proceedings of *1994 International Compressor Engineering Conference at Purdue* (Ed W. Soedel), Purdue University, West Lafayette, Indiana, Vol. 1, 1994, 55-60.

15 **Fleming, J.S., Tang, Y.** and **Anderson, H.** Twin screw compressor performance and its relationship with rotor cutter blade shape and manufacturing cost. In Proceedings of *1994 International Compressor Engineering Conference at Purdue* (Ed W. Soedel), Purdue University, West Lafayette, Indiana, Vol. 2, 1994, 647-652.

16 **Sjöholm, L.** Different operational modes for refrigeration twin-screw compressors. In Proceedings of *1986 International Compressor Engineering Conference at Purdue* (Eds J.F. Hamilton and R. Cohen), Purdue University, West Lafayette, Indiana, Vol. 1, 1986, 89-104.

17 **Mori, H., Kasuya, K., Fujiwara, M., Matsubara, K., Suzuki, A.** and **Aoki, M.** Single stage, oil-free screw compressor with a compression ratio of eight. In Proceedings of *1986 International Compressor Engineering Conference at Purdue* (Eds J.F. Hamilton and R. Cohen), Purdue University, West Lafayette, Indiana, Vol. 1, 1986, 105-118.

18 **Tang, Y.** and **Fleming J.S.** Simulation of working process of an oil flooded helical screw compressor with liquid refrigerant injection. In Proceedings of *1992 International Compressor Engineering Conference at Purdue* (Ed J.F. Hamilton), Purdue University, West Lafayette, Indiana, Vol. 1, 1992, 213-220.

19 **Tang, Y.** and **Fleming J.S.** Obtaining the optimum geometrical parameters of a refrigeration helical screw compressor. In Proceedings of *1992 International Compressor Engineering Conference at Purdue* (Ed J.F. Hamilton), Purdue University, West Lafayette, Indiana, Vol. 1, 1992, 221-227.

20 **Miyoshi, K.** Analysis of screw compressor performance based on indicator diagrams. In Proceedings of *1992 International Compressor Engineering Conference at Purdue* (Ed J.F. Hamilton), Purdue University, West Lafayette, Indiana, Vol. 1, 1992, 259-268.

21 **Kangping, C., Zhenwu, T.** and **Hengyi, C.** The development and application of a water-injected twin screw compressor. In Proceedings of *1992 International Compressor Engineering Conference at Purdue* (Ed J.F. Hamilton), Purdue University, West Lafayette, Indiana, Vol. 1, 1992, 269-278.

22 **Adams, G.P.** and **Soedel, W.** A method for computing the compression loads in twin screw compressors. In Proceedings of *1994 International Compressor Engineering Conference at Purdue* (Ed W. Soedel), Purdue University, West Lafayette, Indiana, Vol. 1, 1994, 67-72.

23 **Adams, G.P.** and **Soedel, W.** Dynamic simulation of rotor contact forces in twin screw compressors. In Proceedings of *1994 International Compressor Engineering Conference at Purdue* (Ed W. Soedel), Purdue University, West Lafayette, Indiana, Vol. 1, 1994, 73-78.

24 **Adams, G.P.** and **Soedel, W.** Computation of Compression Loads in Twin Screw Compressors. *ASME Journal of Mechanical Design*, Vol. **117**, (1995), 512-519.

25 **Huttebraucker, D., Puchas, C., Fick, W.** and **Joos, K.** Entwicklungskonzept des Mercedes-Benz-Vierzylinder-Ottomotors mit mechanischer Aufladung für die C-Klasse. *MTZ*, No **56** Dec 95, 772-775.

26 **Huttebraucker, D., Puchas, C., Fick, W.** and **Joos, K.** Development of the Mercedes-Benz 4-Cylinder Gasoline Engine with Compressor. In Proceedings of *VDI-Internationales Wiener Motorensymposium*, 25-26 April 1996, 69-95.

27 **Schmitz, T., Holloh, K.D.** and **Jurgens, R.** Potentiale einer mechanischen Zusatzaufladung für Nutzfahrzeugmotoren. *MTZ*, No **55** May 94, 309-315.

28 **Mimmi, G.** and **Pennacchi, P.** Computation of rotor loads in three screw pumps. To be printed on *ASME Journal on Mechanical Design*.

29 **Sesini, O.** *Meccanica Applicata alle Macchine – Cinematica*. Vol.**1**, Casa Editrice Ambrosiana, Milan, Italy.

30 **Mimmi G.** and **Pennacchi P.** Flow Rate Regularity in Rotary Trochoidal-Lobe Pumps. *Machine Elements and Machine Dynamics*, G.R. Pennock ed., DE-Vol.**71**, 1994, The American Society of Mechanical Engineering, New York, 295-302.

31 **Mimmi, G.** and **Pennacchi, P.** Design of three-screw positive displacement rotary pumps. *Contact Mechanics II - Computational Techniques*, M.H. Aliabadi and C. Alessandri eds., 1995, Computational Mechanics Publications, Southampton Boston.

32 **Mimmi, G.** and **Pennacchi, P.** Determination of Tool Profile for the Milling of Three Screw Pump Rotor. *Meccanica - International Journal of the Italian Association of Theoretical and Applied Mechanics*, Vol **32**, no 4, 1997, 363-376.

33 **Henriot, J.** *Ingranaggi: trattato teorico e pratico*. Tecniche Nuove, Milano, 1987.

34 **Amerio, L.** *Analisi Matematica*. vol.1, UTET, Torino, 1986.